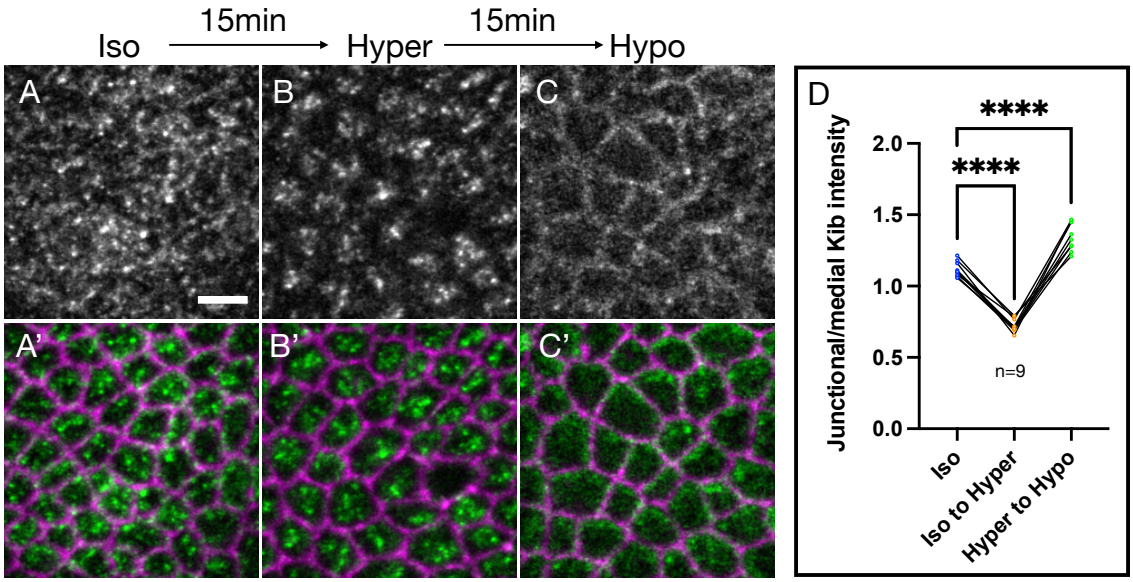
Iso
15min
Hyper
15min
Hypo
A
B
C
A'
B'
C'
D
Junctional/medial Kib intensity
2.0
1.5
1.0
0.5
0.0
****
****
n=9
Iso
Iso to Hyper
Hyper to Hypo

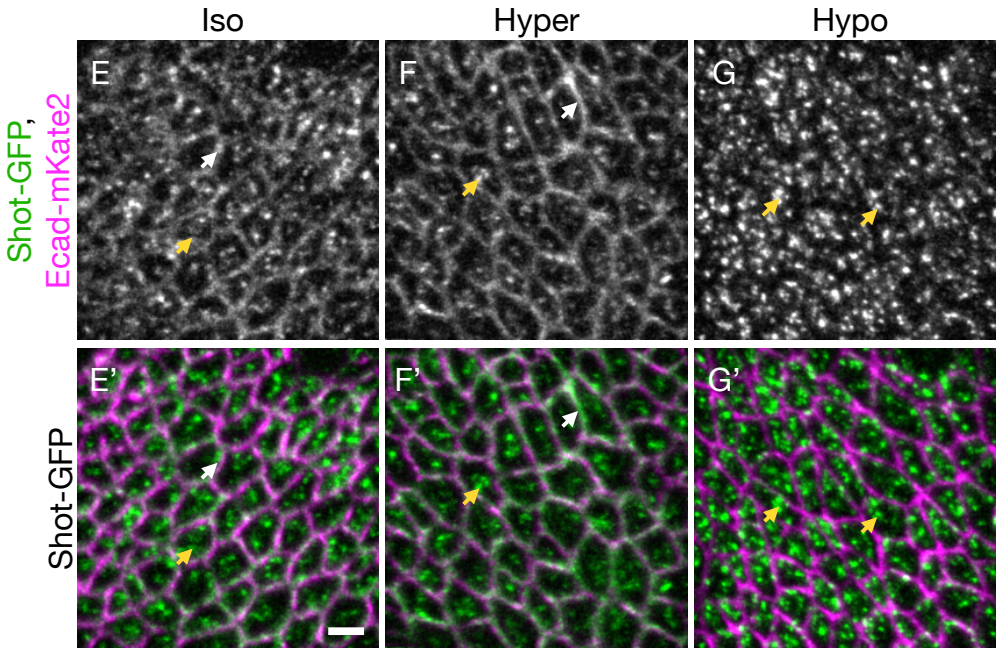
Iso
Hyper
Hypo
Shot-GFP, Ecad-mKate2
Shot-GFP
E
F
G
E'
F'
G'

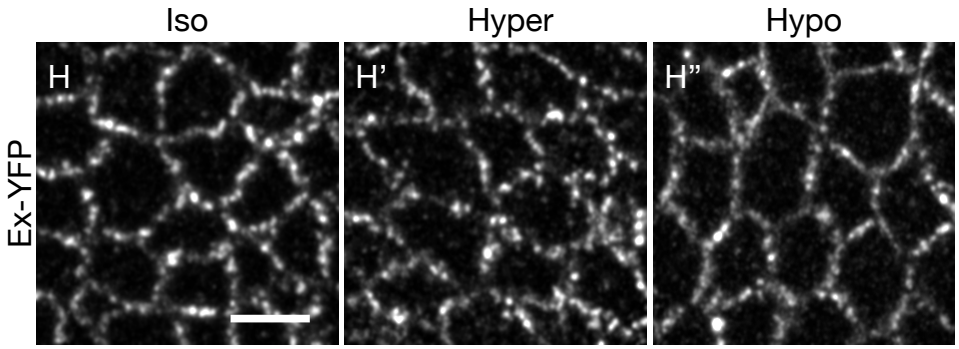
Iso
Hyper
Hypo
Ex-YFP
H
H'
H''

Figure S1, related to Figure 2.
The effect of osmotic shifts on Kib localization is specific.
(A-C) The effects of osmotic shifts are reversible. Shifting a wing imaginal tissue from isotonic (A and A') to hypertonic (B and B') solution leads to medial Kib accumulation. Shifting the same tissue from hypertonic to hypotonic (C and C') conditions results in redistribution of Kib from the medial to the junctional cortex.
(D) Quantification of junctional/medial Kib distribution in tissues sequentially subjected to isotonic to hypertonic followed by hypertonic to hypotonic shifts. Statistical significance was calculated using Repeated Measures one-way ANOVA test; n = number of wing discs.
(E-G') Similar to Kib, Shot localizes at the junctional (white arrow) and medial cortex (yellow arrowhead) under isotonic conditions (A and A'). However, Shot remains both junctional and medial under hypertonic conditions (B and B') and becomes predominantly medial under hypotonic conditions (C and C').
(H-H'') Unlike Kib, Ex remains mostly junctional under osmotic shifts. Scale bars = 3μm.

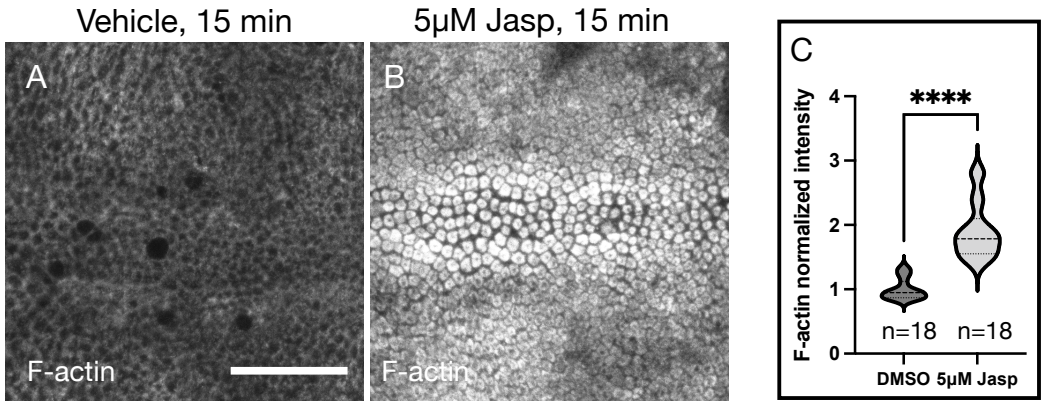
Vehicle, 15 min
5μM Jasp, 15 min
A
B
F-actin
F-actin
C
F-actin normalized intensity
****
n=18
n=18
DMSO
5μM Jasp

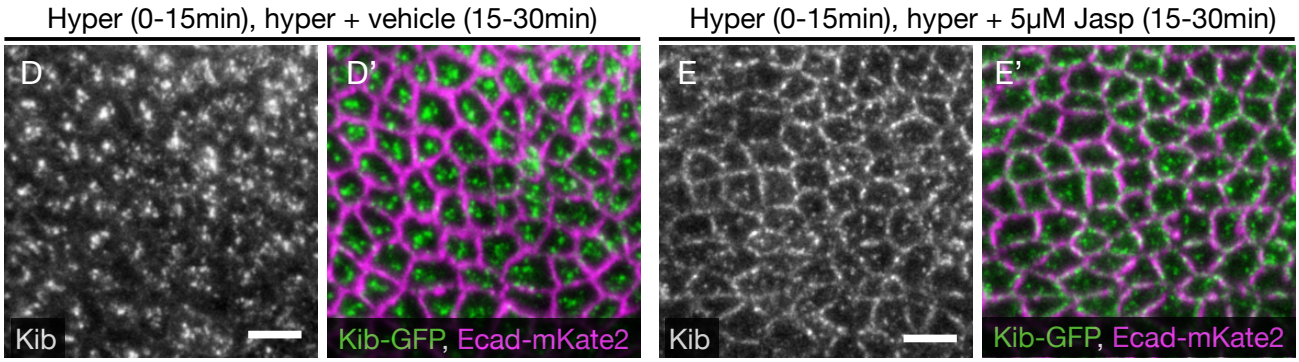
Hyper (0-15min), hyper + vehicle (15-30min)
Hyper (0-15min), hyper + 5μM Jasp (15-30min)
D
D'
E
E'
Kib
Kib-GFP, Ecad-mKate2
Kib
Kib-GFP, Ecad-mKate2

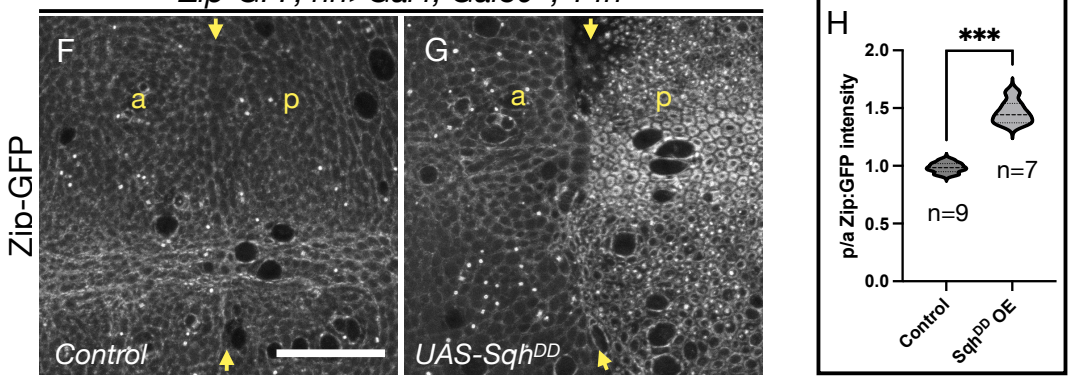
Zip-GFP, hh>Gal4, Gal80ts, 14h
Zip-GFP
F
G
a
p
a
p
Control
UAS-SqhDD
H
***
p/a Zip:GFP intensity
n=9
n=7
Control
SqhDD OE

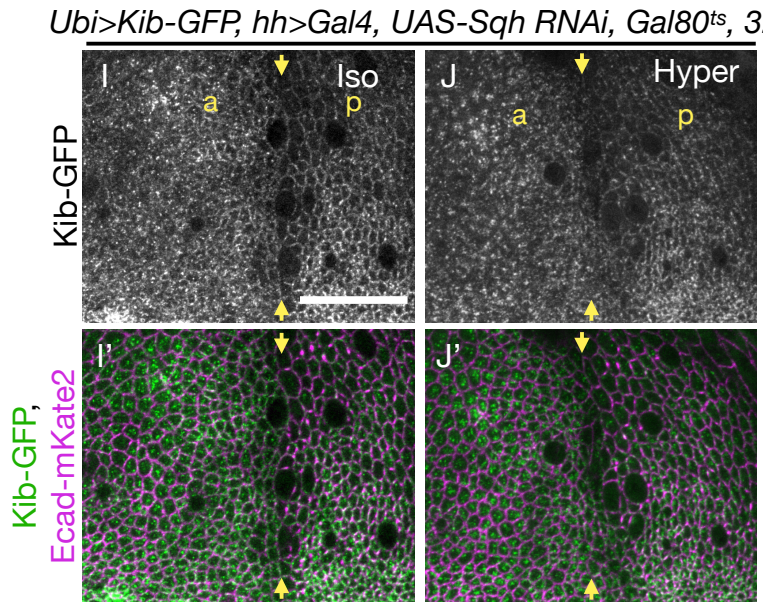
Ubi>Kib-GFP, hh>Gal4, UAS-Sqh RNAi, Gal80ts, 32h
Kib-GFP
Kib-GFP, Ecad-mKate2
I
Iso
J
Hyper
a
p
a
p
I'
J'

Figure S2, related to Figure 3.
Medial Kib accumulation is mediated via actomyosin dynamics.
(A and B) Compared to control tissues (A), F-actin (sGMCA) was more stabilized in tissues treated with 5µM Jasp (B). Scale bar = 20µm.
(C) Quantification of mean sGMCA intensity in tissues treated with DMSO or 5µM Jasp. Statistical significance was calculated using Mann-Whitney test; n = number of wing discs.
(D-E') F-actin dynamics are required to maintain Kib at the medial cortex. Tissues were first incubated under plain hypertonic conditions for 15 min to concentrate Kib medially, and then transferred to a hypertonic medium with DMSO (D and D') or 5µM Jasp (E and E'). Treatment with 5µM Jasp reverses medial Kib accumulation (E and E'). Scale bar = 5µm.
(F-G) Compared to control tissues (F), transient ectopic expression of Sqh^{DD} in the posterior compartment of the wing disc results in significant stabilization of the myosin heavy chain, Zip-GFP (G). Yellow arrows indicate the anterior-posterior (a-p) boundary. Scale bar = 20µm.
(H) Quantification of the posterior/anterior (p/a) mean Zip:GFP intensity in control tissues and tissues transiently expressing Sqh^{DD} in the posterior compartment. Statistical significance was calculated using Mann-Whitney test; n = number of wing discs.
(I-J') Transient depletion of Sqh in the posterior compartment of the wing imaginal disc leads to more junctional Kib (I and I') and prevents medial Kib accumulation under hypertonic conditions (J and J'). Scale bar = 20µm.

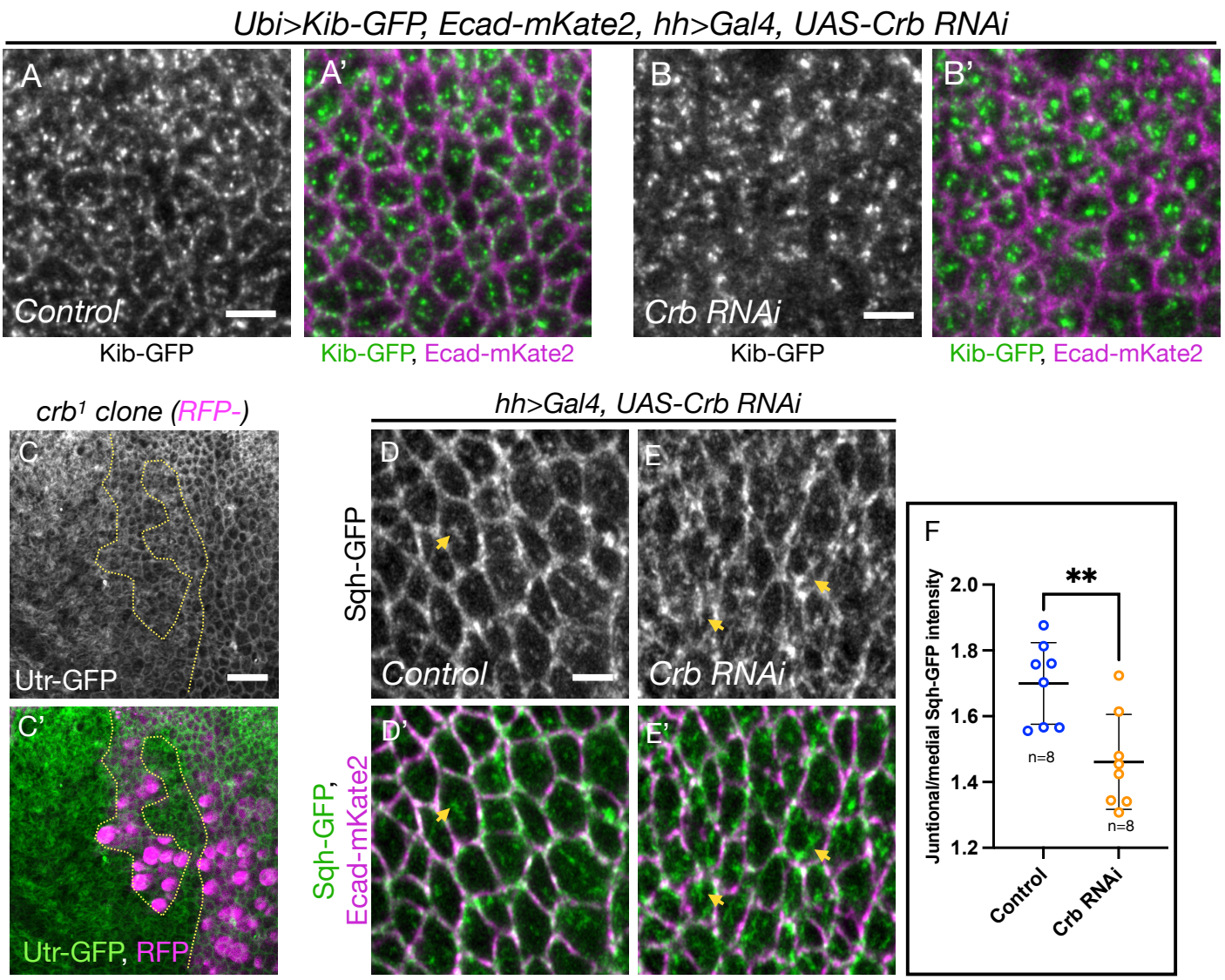
Ubi>Kib-GFP, Ecad-mKate2, hh>Gal4, UAS-Crb RNAi
A
Control
Kib-GFP
A'
Kib-GFP, Ecad-mKate2
B
Crb RNAi
Kib-GFP
B'
Kib-GFP, Ecad-mKate2
crb¹ clone (RFP-)
C
Utr-GFP
C'
Utr-GFP, RFP
hh>Gal4, UAS-Crb RNAi
Sqh-GFP
D
Control
E
Crb RNAi
Sqh-GFP, Ecad-mKate2
D'
E'
F
Juntional/medial Sqh-GFP intensity
2.0
1.8
1.6
1.4
1.2
**
n=8
n=8
Control
Crb RNAi
hh>Gal4, UAS-Crb RNAi
Ubi>Kib-GFP
G
a
p
Vehicle
H
a
p
5μM Jasp
Ubi>Kib-GFP, Ecad-mKate2
G'
a
p
H'
a
p

Figure S3, related to Figure 3 and Figure 5.
Crb regulates Kib localization via actomyosin dynamics and junctional tethering.
(A-B') Kib is junctional and medial in control cells (A and A') but is more medial in cells depleted of Crb (B and B'). Scale bar = 5µm.
(C and C') Apical F-actin organization is more medial in crb^{1} somatic mosaic clones. Scale Bar = 10µm.
(D-E') Compared to control cells (D and D'), cells depleted of Crb (E and E') display disrupted junctional myosin organization and more pronounced medial myosin accumulation (arrowheads). Scale Bar = 3µm.
(F) Quantification of junctional/medial myosin distribution in control vs. Crb-depleted cells. Statistical significance was calculated using the Mann-Whitney test; n = number of wing discs.
(G-H') Although Kib accumulates medially upon depletion of Crb in the posterior (p) compartment of the wing imaginal disc (G and G'), this accumulation is blocked by Jasp treatment (H and H'). Note that while Jasp treatment enhances junctional Kib localization in the anterior (a) compartment, it fails to restore junctional Kib in the posterior, where Crb is depleted (H and H'). Scale Bar = 10µm.

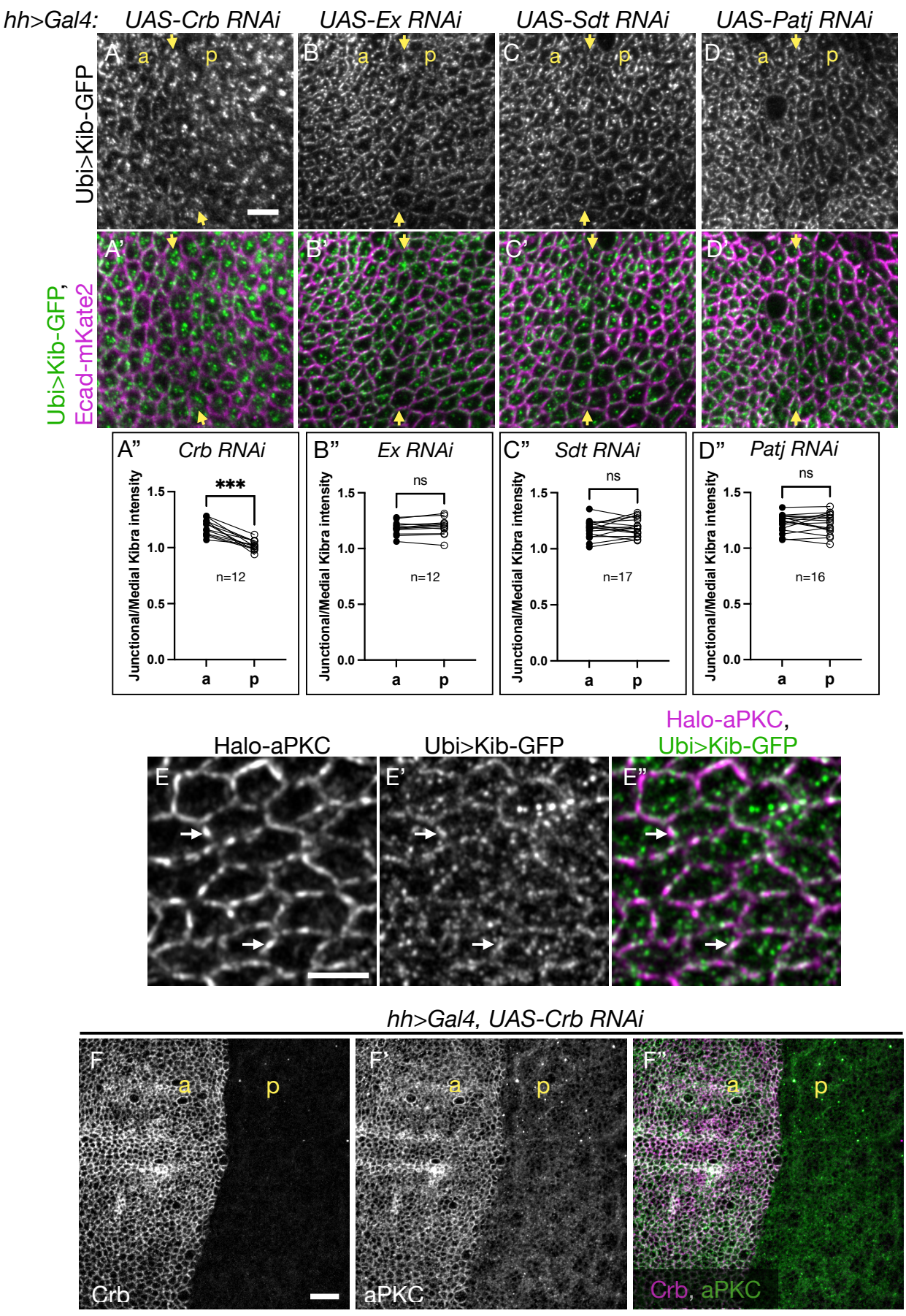
hh>Gal4:
UAS-Crb RNAi
UAS-Ex RNAi
UAS-Sdt RNAi
UAS-Patj RNAi
Ubi>Kib-GFP
Ubi>Kib-GFP;
Ecad-mKate2
A a p
B a p
C a p
D a p
A'
B'
C'
D'
A" Crb RNAi
B" Ex RNAi
C" Sdt RNAi
D" Patj RNAi
Junctional/Medial Kibra intensity
***
ns
n=12
n=12
n=17
n=16
Halo-aPKC
Ubi>Kib-GFP
Halo-aPKC,
Ubi>Kib-GFP
E
E'
E"
hh>Gal4, UAS-Crb RNAi
F
F'
F"
Crb
aPKC
Crb, aPKC

Figure S4, related to Figure 5 and Figure 6.
Crb does not control Kib localization via Ex, Sdt, or Patj.
A-D'') While loss of Crb results in more medial Kib (A-A''), loss of Ex (B-B''), Sdt (C-C''), or Patj (D-D'') has no significant effect on Kib localization. Yellow arrowheads indicate the anterior-posterior (a-p) boundary. Scale bar = 5μm.
Statistical significance was calculated using Wilcoxon matched-pairs signed rank test; n = number of wing discs.
E-E'') An apical projection of the wing imaginal disc cells showing that aPKC is highly enriched at the junctional cortex and that some junctional aPKC foci co-localize with Kib (white arrows). Scale bar = 3μm.
F-F'') Crb depletion in the posterior (p) compartment of the wing imaginal disc leads to significant decrease in cortical aPKC. Scale bar = 10μm.

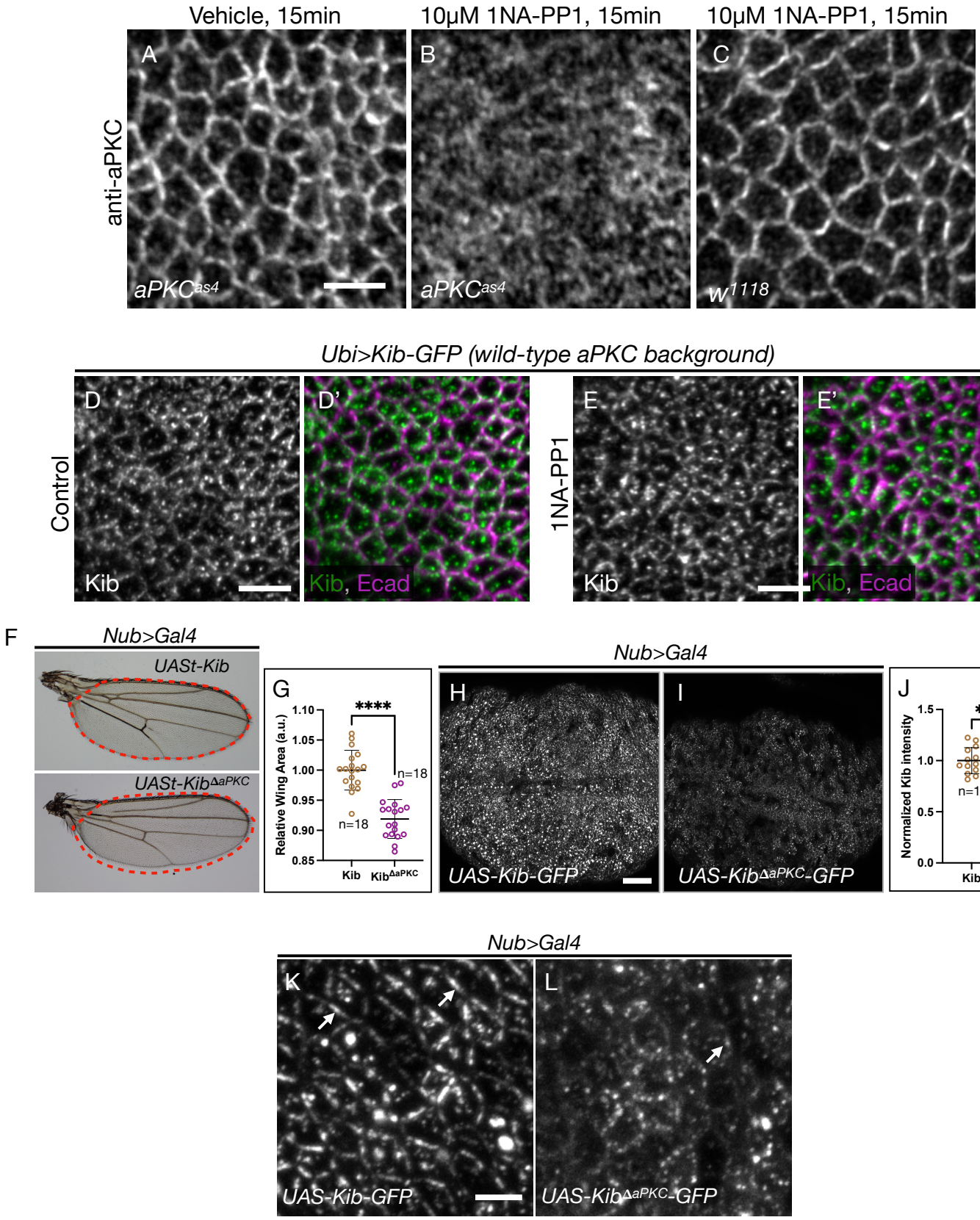
Vehicle, 15min
10μM 1NA-PP1, 15min
10μM 1NA-PP1, 15min
anti-aPKC
A
B
C
aPKCas4
aPKCas4
w1118
Ubi>Kib-GFP (wild-type aPKC background)
Control
1NA-PP1
D
D'
E
E'
Kib
Kib, Ecad
Kib
Kib, Ecad
F
Nub>Gal4
UASt-Kib
UASt-KibΔaPKC
G
Relative Wing Area (a.u.)
1.10
1.05
1.00
0.95
0.90
0.85
****
n=18
n=18
Kib
KibΔaPKC
Nub>Gal4
H
I
UAS-Kib-GFP
UAS-KibΔaPKC-GFP
J
Normalized Kib intensity
1.5
1.0
0.5
0.0
****
n=14
n=13
Kib
KibΔaPKC
Nub>Gal4
K
L
UAS-Kib-GFP
UAS-KibΔaPKC-GFP

Figure S5, related to Figure 7.
aPKC-mediated regulation of Kib in vivo.
(A-C) Validation of the specificity of aPKC^{as4} inhibition by 1NA-PP1 in the wing imaginal disc. In tissues homozygous for *aPKCas4* allele, aPKC displays normal cortical localization (A). Treatment with 1NA-PP1 severely disrupts aPKC cortical localization (B). In contrast, wild-type aPKC is not affected by 1NA-PP1 treatment (C). Scale bar = 5µm.
(D-E') Treatment with 1NA-PP1 does not affect Kib localization in the wild-type *aPKC* background. Scale bars = 5µm.
(F and G) Ectopic expression of Kib$^{\Delta aPKC}$ (*UASt>Kib$^{\Delta aPKC}$-GFP*) using a wing-specific driver (*Nub>Gal4)* leads to slightly smaller wings compared to the expression of wild-type Kib (*UASt>Kib-GFP*); n = number of wings.
(H-J) Wild-type Kib (H) ectopically expressed specifically in the wing pouch is more stable than Kib$^{\Delta aPKC}$ (I and J); n = number of wing discs. Scale bar = 20µm. Transgenes in F-I are identically expressed.
Statistical significance in (G) and (J) was calculated using Mann-Whitney test.
(K-L) Similar to wild type Kib-GFP, ectopically expressed Kib$^{\Delta aPKC}$-GFP still localizes at the junctional cortex, albeit less prominently. Note that brightness in L was enhanced relative to K. Scale bar = 3µm.

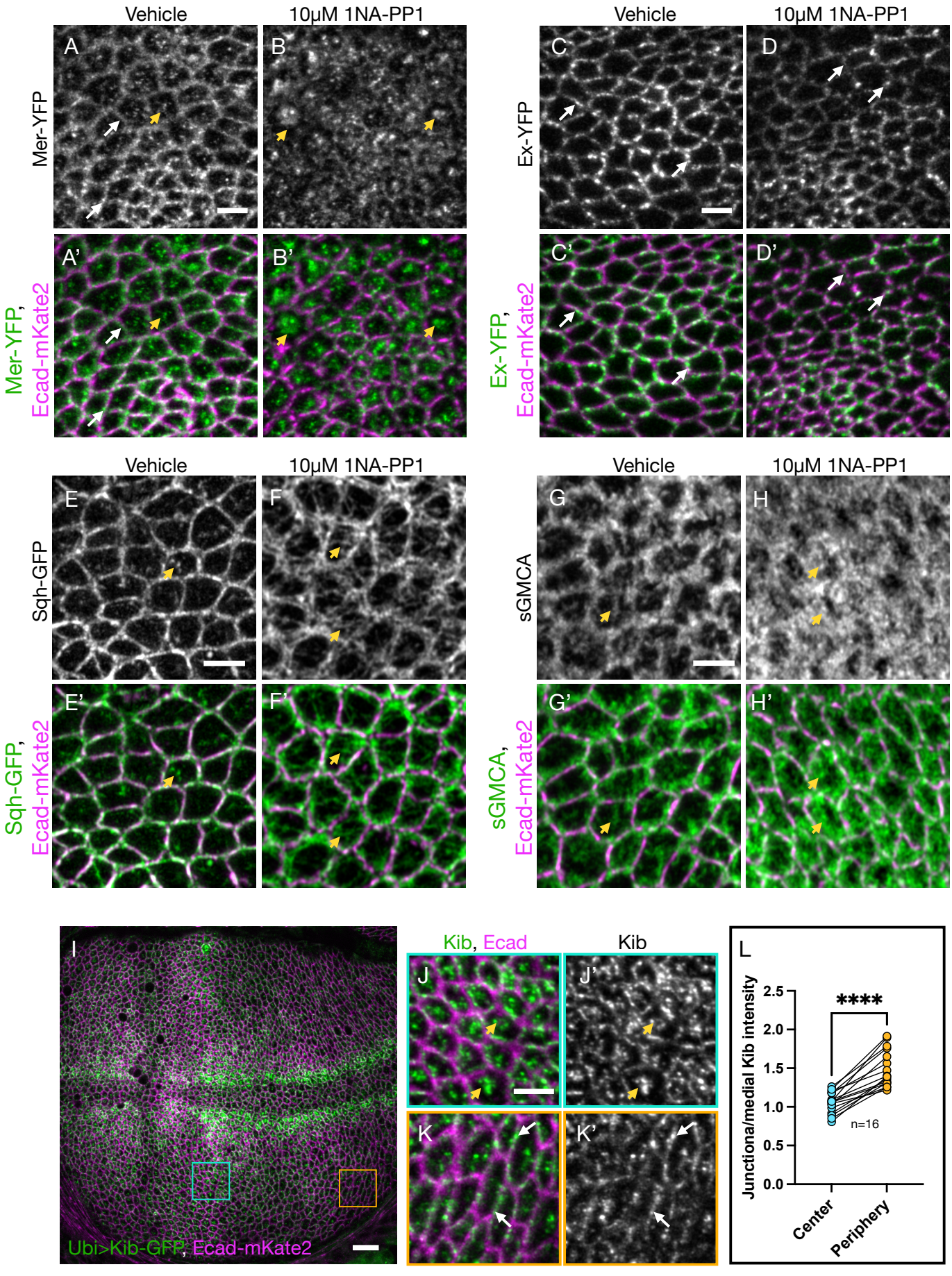
Vehicle
10μM 1NA-PP1
Mer-YFP
Mer-YFP, Ecad-mKate2
Ex-YFP
Ex-YFP, Ecad-mKate2
Sqh-GFP
Sqh-GFP, Ecad-mKate2
sGMCA
sGMCA, Ecad-mKate2
Ubi>Kib-GFP, Ecad-mKate2
Kib, Ecad
Kib
Junctional/medial Kib intensity
****
n=16
Center
Periphery

Figure S6, related to Figure 7.
The effect of acute aPKC inhibition on Hippo pathway components and actomyosin organization.
(A-B') Compared to control conditions (A and A') where Mer displays junctional and medial localization, Mer becomes more medial under aPKC inhibition with 1NA-PP1 (B and B').
(C-D') Unlike Kib and Mer, Ex remains junctional under aPKC inhibition with 1NA-PP1.
(E-H') aPKC inhibition with 1NA-PP1 results in more medial myosin (E-F') and F-actin (G-H') organization. Wing imaginal tissues in A-H' are homozygous for *aPKCas4* allele. Scale bars = 3μm.
(I) A low magnification view of a wing imaginal tissue expressing Ubi>Kib-GFP and Ecad-mKate2. The boxes indicate the regions at the center (cyan) and the periphery (orange) of the tissue that are enlarged in (J-K'). Scale bar = 10μm.
(J-K') Enlarged views of cells at the center (J and J') and periphery (K and K') of the tissue shown in (I). Scale bar = 3μm. Yellow arrowheads point to the medial cortex; white arrows point to the junctional cortex.
(L) Quantification of mean junctional/medial Kib intensity in cells at the center vs. periphery of the wing imaginal epithelium. Statistical significance was calculated using Wilcoxon matched-pairs signed rank test; n = number of wing discs.